


## Scaling to zero of compressive modulus in disordered isostatic cubic networks

Cristian F. Moukarzel <sup>\*</sup>*Depto. de Física Aplicada, CINVESTAV del IPN, Av. Tecnológico Km 6, 97310 Mérida, Yucatán, México*Gerardo G. Naumis *Depto. de Sistemas Complejos, Instituto de Física, Universidad Nacional Autónoma de México (UNAM),  
Apdo. Postal 20-364, 01000, CDMX, México*

(Received 31 October 2021; revised 12 August 2022; accepted 9 September 2022; published 30 September 2022)

Networks with as many mechanical constraints as degrees of freedom and no redundant constraints are minimally rigid or isostatic. Isostatic networks are relevant in the study of network glasses, soft matter, and sphere packings. Because of being at the verge of mechanical collapse, they have anomalous elastic and dynamical properties not found in the more commonly occurring hyperstatic networks. In particular, while hyperstatic networks are only slightly affected by geometric disorder, the elastic properties of isostatic networks are dramatically altered by it. In this paper, we show how disorder and system size strongly affect the ability of isostatic networks to sustain a compressive load. We develop an analytic method to calculate the bulk compressive modulus  $B$  for various boundary conditions as a function of disorder strength and system size. For simplicity, we consider square and cubic lattices with  $L^d$  sites, each having  $d$  mechanical degrees of freedom, and  $dL^d$  rotatable springs in the presence of hot-solid disorder of magnitude  $\epsilon$ . Additionally,  $\sim L^\theta$  sites may be fixed, thus introducing a nonextensive number of redundancies, either in the bulk or on the boundaries of the system. In all cases,  $B$  is analytically and numerically shown to decay as  $L^{-\mu}$  with  $\mu_{\text{large}} = d - \theta$  for large disorder and  $\mu_{\text{small}} = \max\{(d - \theta - 1), 0\}$  for small disorder. Furthermore  $B(L, \epsilon)L^{\mu_{\text{small}}} = g(\lambda)$  with  $\lambda = L^{(\mu_{\text{large}} - \mu_{\text{small}})\epsilon^2}$  a scaling variable such that  $\lambda \ll 1$  is small disorder and  $\lambda > 1$  is large disorder. The faster decay to zero of  $B$  in the large disorder regime results from a broad distribution of spring tensions, including tensions of both signs in equal proportions, which is remarkable since the system is under a purely compressive load. Notably, the bulk modulus is discontinuous at  $\epsilon = 0$ , a consequence of the fact that the regular network sits at an unstable degenerate configuration.

DOI: [10.1103/PhysRevE.106.035001](https://doi.org/10.1103/PhysRevE.106.035001)

### I. INTRODUCTION

The balance [1] between numbers of degrees of freedom and mechanical constraints is a central keystone in the analysis of structural rigidity [2]. Rigid properties are also important at the atomic scale in several fields of physics such as glasses, soft matter, sphere packings, protein folding, etc. [3,4]. Balanced, or isostatic, networks are minimally rigid and thus at the verge of mechanical collapse. Their elastic and dynamical properties are not well understood [5]. In particular, there is a scarcity of studies discussing the effects of size and disorder strength [6,7] on isostatic networks. Here we present an analytical method that sheds light on such questions for the case of cubic networks and admits easy generalization to other kinds of isostatic lattices. Our analytical results are validated through extensive numerical simulations.

The elastic properties of network-forming systems can be modeled for simplicity using spring-joint networks in  $d$  dimensions. In these simplified models, each pointlike node has  $d$  positional degrees of freedom, while each rotatable spring

determines the distance between two joints, thus providing one constraint [8–10]. In general, however, the counting of degrees of freedom and constraints depends upon the interactions between nodes. In covalently bonded three-dimensional atomic systems, each atom has six degrees of freedom, while each covalent bond provides five constraints. Similarly, in a cubic spring network with nonrotatable springs that are solidly attached to nodes [11–13], each node has six degrees of freedom while each spring provides six constraints.

Networks with too few mechanical constraints are flexible or hypostatic, and may be deformed without energy expenditure. A mode of deformation that costs no energy is called a *flex*. Networks with more constraints than required for rigidity are overconstrained or hyperstatic and can sustain self-stresses. Self-stresses, also called *cycles*, are sets of link tensions in equilibrium without external forces. Networks that have just the number and positioning of constraints needed for minimal rigidity are called isostatic and have neither flexes nor cycles. They are minimally rigid in the same sense as trees are minimally connected [14]: removing any single link renders some subset of the network not rigidly connected to the rest. Because the problems of finding spring tensions from external forces and that of finding joint positions form spring

<sup>\*</sup>cristian.moukarzel@cinvestav.mx

lengths are both uniquely determined, such well-balanced networks are also said to be statically and kinematically determinate [15].

Notably, the same mechanical arguments determining the rigidity of load-bearing structures are relevant at atomic scales as well, e.g., regarding the dynamics of covalently bonded glass-forming fluids, as noticed by Phillips [3]. Phillips observed that the glass-forming ability of a melt is maximized when its chemical composition is such that the number of mechanical atomic degrees of freedom is exactly saturated by the hard constraints provided by covalent bonds. It was then suggested that such mechanically balanced random covalent networks would be rigid but nearly stress-free [16]. Further work by Thorpe [17,18] tried to conceptualize these observations in the context of random rigidity percolation (RRP) [19], which then remained a predominant model in the study of rigidity-related properties of covalent glass formers [20]. According to the then-accepted picture, the single observed maximum in glass-forming ability as the chemical composition is varied would correspond to the single second-order transition in RRP.

However, RRP never gives rise to rigid and stress-free, that is, isostatic, networks. Fluctuations in local connectivity create self-stressed regions [21] intermixed with underconstrained or floppy regions [22], even if constraint balance is satisfied globally. Constraint balance is a necessary but not sufficient condition for isostaticity. The spontaneous assembly of a rigid and stress-free, or isostatic, structure requires some mechanism by which self-stresses are avoided as the network connectivity is increased toward the rigidization point. The first known example of a naturally occurring system in which such a mechanism exists, and thus self-organizes onto an isostatic structure, was provided by packings of frictionless elastic disks or spheres [4], which is a model for metallic glasses [23].

In the meantime, Boolchand found experimental evidence indicating that certain network glass formers show not one but two rigidity transitions as a function of chemical composition, with an intermediate phase displaying almost no aging, a minimum in nonreversible heat flow, and improved glass formation ability [24,25]. These properties of the intermediate phase are consistent with the suppression of self-stress, and could not be explained by the then-prevalent RRP model. Subsequently, Thorpe and Phillips proposed a modified rigidity percolation model [26,27] in which, by assuming that excess constraints are avoided on energy minimization grounds, two structural transitions are obtained, giving rise to an intermediate phase that is rigid and nearly stress-free, thus providing a possible conceptual framework for Boolchand *et al.*'s experimental findings [28].

The discovery of self-organized isostaticity in sphere packings [4] and network glasses [26,27] brought about interest in the study of isostatic networks and their relevance in natural systems, particularly glasses. Recently, it was argued by Wyart and collaborators [5,29] that the excess density of low-energy vibrational modes observed in amorphous systems, i.e., the boson peak [30], can be explained as being a consequence of a proliferation of soft modes that is characteristic of isostatic networks. Soft, or floppy modes, are deformations which cost little elastic energy, and are thus associated with

a small vibrational frequency. Its importance for the glass transition phenomenology and phase transitions is now well established [31–33].

There are, however, important structural differences between network glasses and sphere packings. In packings, contact forces cannot be tensile. This condition, on one hand, implies that no localized self-stresses are possible, from which a rigorous proof of isostaticity [4] can be constructed. In network glasses, on the other hand, isostaticity is hypothetical. Its theoretical justification is based on self-stress minimization, a mechanism that may or may not be at work, depending on the glass-formation conditions [34]. But, more importantly, the property of compressive tensions in packings ensures that their bulk modulus is nonzero [5]. The condition of compressivity of contact forces implies that disorder in random packings is not uncorrelated. Precise correlations exist among the disorder variables of a packing, e.g., sphere positions and contacts, to ensure that no link force is tensile. In random isostatic networks such as those that are thought to exist in network glasses, bond forces can have any sign. Therefore, no such correlations exist, and link forces will grow with size upon loading, giving rise to negligible elastic moduli for these systems [35,36]. This is why randomly disordered isostatic networks cannot be used [6,7] as models for the static elastic properties of compressive packings. But randomly disordered isostatic networks, on the other hand, constitute adequate models to represent network glasses, which do not have a constraint on tension signs that would impose correlations on the disorder variables.

In previous work, we have studied how static response functions [37–39] and elastic moduli [35] behave in propagative isostatic networks that possess geometric disorder. These studies clearly show that many anomalous elastic properties of isostatic networks only manifest themselves in the presence of disorder. The physical properties of disordered isostatic networks, therefore, will in general strongly depart from those of their regular counterparts, something that does not happen in hyperstatic networks.

In this paper, we investigate how random site displacements of magnitude  $\epsilon$  (hot-solid disorder [40]) affect the ability of square and cubic networks, which are isostatic if connected via rotatable springs, to withstand an isotropic compressive load. It is important to once again remark that this strong sensitivity to disorder does not exist in hyperstatic systems. For comparison, consider cubic networks whose nodes are solidly joined by nonrotatable springs [11–13]. As mentioned already, such systems have more mechanical constraints than node degrees of freedom, and therefore they are not isostatic but redundantly rigid or hyperstatic. Their elastic properties are almost unchanged in the presence of disorder [12]. Although our focus is on square and cubic networks, similar conclusions are valid for other regular isostatic networks with a finite compressive modulus, e.g., Kagome [41]. Finally, notice that hot-solid disorder provides an approximate static description for the effects of thermal fluctuations on elastic response [42,43], particularly at low temperatures, where entropic effects are not important.

Previous numerical studies [36] of the compressive modulus  $B$  of square networks with hot-solid disorder [40] of magnitude  $\epsilon$  revealed the following remarkable properties.

For regular ( $\epsilon = 0$ ) square networks with periodic boundary conditions (PBCs), the bulk modulus is constant,  $B = 1$ , for any size  $L$ . For any nonzero  $\epsilon$ , however,  $B$  decreases with increasing linear system size  $L$  as  $1/L$  if  $\epsilon^2 L \ll 1$ , and as  $1/L^2$  if  $\epsilon^2 L > 1$ . The bulk modulus  $B$  is thus discontinuous at  $\epsilon = 0$ , for any size  $L$ .

Additionally, the equilibrium deformation  $\langle (\delta\vec{r})^2 \rangle^{1/2}$  under load is found to *diverge* as  $1/\epsilon$  in the  $\epsilon \rightarrow 0$  limit, although it is exactly zero for  $\epsilon = 0$ . The square network with PBCs is, within linear elasticity, mechanically unstable in the following sense: A large regular network with  $\epsilon = 0$  has a finite bulk modulus, and its sites remain unmoved under isotropic compression, but the slightest amount of initial deformation  $\epsilon \neq 0$  renders it unable to withstand a load: the elastic modulus goes to zero with size and its sites suffer enormous displacement, actually diverging as  $1/\epsilon$ . Notice that this, being a statement that holds within linear elasticity, is equally valid for compression and extension of the network. The instability of these networks under site disorder is, therefore, not equivalent to the buckling of a compressed elastic element, which is a higher-order effect, does not require disorder, and most importantly does not happen under extension. These particularities of square networks with PBCs derive from the existence of degenerate flexes [44], or zero-energy deformabilities, at  $\epsilon = 0$ .

Isostatic networks with fixed boundaries, on the other hand, do not possess such flexes, and display a rather different behavior. They have a constant bulk modulus as  $\epsilon \rightarrow 0$ , and their average equilibrium deformation under compression goes to zero as  $\epsilon$  in that limit. Furthermore, their elastic modulus decays as  $1/L$  for large  $\epsilon$ .

Imposing fixed boundaries amounts to fixing two perpendicular lines of site in two dimensions, and three planes of site in three dimensions, network with periodic boundaries. In other words, fixing  $\sim L^{(d-1)}$  sites of a  $d$ -dimensional network. In this paper, we consider the more general case of cubic and square systems with periodic boundaries, in which  $\sim L^\theta$  sites are fixed, where the scaling dimension of fixed sites satisfies  $0 \leq \theta \leq d$ . The density of overconstraints is thus asymptotically zero, so all networks that we analyze will be said to be asymptotically isostatic.

We analytically derive the bulk modulus  $B$  of such networks as a function of model parameters  $L$  (linear size),  $\epsilon$  (disorder strength), and  $\theta$  (scaling dimension of fixed sites). For this purpose, the bulk modulus  $B$  is written in terms of the number  $N_{\text{cycles}}$  and size  $M_c$  of cycles, i.e., subgraphs of the network that can carry self-stress, plus some approximate knowledge of the relative variability  $\nu$  of stresses in these cycles. The number and size of cycles on cubic and square cycles with  $L^\theta$  fixed sites can be easily estimated. The dependence of  $\nu$  on disorder is not exactly known, but can be adequately guessed in the limits of large and small disorder, so an analytic expression for  $B$  as a function of model parameters can be found. The validity of these analytic results is then verified numerically by solving the elastic equations with the help of a conjugate gradient [45] iterative procedure for square and cubic networks.

The layout of this paper is as follows. Section II details the procedure by which the compressive modulus is

calculated. Starting from a general expression for  $B$  [5] derived in Appendix A, we use approximations that are appropriate for square and cubic networks, arriving at Eq. (3), which gives the bulk modulus  $B$  in terms of geometric properties of self-stressed subgraphs (or cycles) and the variability of the tensions they sustain.

In Sec. III these geometric properties of cycles are determined for the particular case under scrutiny, that is, disordered square and cubic networks, using graph-rigidity notions enumerated in Appendix B. These results are then used to find the bulk modulus  $B$  in the various cases under consideration. The relationship between the bulk modulus decay exponent  $\mu$  and the scaling dimension  $\theta$  of the number constraints in excess of minimal rigidity is given by (16).

Section IV explains our numerical methodology and presents our numerical results for square and cubic networks. It is discussed here how our numerical results validate our analytical predictions. It is also shown in this section that  $B(L, \epsilon)$  times an appropriate power of size can be written as a function of a single scaling variable  $\lambda$  that depends on size  $L$  and disorder  $\epsilon$ , and separates the regimes of small and large disorder. Finally, Sec. V offers a discussion of our results, open questions, and future work.

## II. DISORDERED CUBIC NETWORKS

We start with a square or cubic network of linear springs with unit lattice spacing and periodic boundaries across all dimensions. As in previous work [35,36], hot-solid disorder [40] is introduced by randomly displacing each site within a sphere of radius  $\epsilon$  and then adjusting all spring lengths  $\ell_s$  so they become unstressed in this configuration. The system is then loaded by isotropically by expanding all springs according to  $\ell_s \rightarrow \ell_s(1 + \kappa)$ , with  $\kappa \ll 1$ . After numerically solving the elastic equations to find the new equilibrium site positions, the bulk modulus is calculated as  $B = \langle n_{ij}^2 \rangle / \langle (\delta\ell)^2 \rangle = \langle n_{ij}^2 \rangle / (\langle \ell_{ij}^2 \rangle \kappa^2)$ , where  $n_{ij}$  is the tension in spring  $ij$ , in equilibrium.

In Appendix A, it is shown that the bulk modulus  $B$  can be written [5] in general as

$$B = \frac{1}{N_{\text{links}}} \sum_{c=1}^{N_{\text{cycles}}} \frac{(\sum_{ij} n_{ij}^c \ell_{ij} / \langle \ell^2 \rangle^{1/2})^2}{\sum_{ij} (n_{ij}^c)^2}, \quad (1)$$

where  $\sum_{ij}$  is a sum over the  $N_{\text{links}}$  springs in the network,  $\sum_{c=1}^{N_{\text{cycles}}}$  is a sum over cycles,  $n_{ij}^c$  is the normalized tension on link  $ij$  in cycle  $c$ , and  $\ell_{ij}$  is the repose length of spring  $ij$ .

We introduce the following approximations, which are valid for slightly disordered regular lattices and may not apply in general. If the link-length variability is not too large, that is if  $\ell_{ij} \approx \langle \ell^2 \rangle^{1/2}$ , we can write

$$B = \frac{1}{N_{\text{links}}} \sum_{c=1}^{N_{\text{cycles}}} \frac{(\sum_{ij} n_{ij}^c)^2}{\sum_{ij} (n_{ij}^c)^2}. \quad (2)$$

Considering now a simple Gaussian approximation for the variability of tensions on a cycle, assume that cycle  $c$  is comprised of  $M_c$  links ( $M_c$  is the mass of cycle  $c$ ) and that link tensions  $n_{ij}^c$  on these links can be described by  $n_{ij}^c = n_c + \sigma_c \xi_{ij}^c$ , with  $\xi_{ij}^c$  a normal random variable. Correlations

in link tensions are ignored. We then have that  $(\sum_{ij} n_{ij}^c)^2 \approx M_c^2 n_c^2 + M_c \sigma_c^2$  and  $\sum_{ij} (n_{ij}^c)^2 \approx M_c (n_c^2 + \sigma_c^2)$ . Therefore,

$$\begin{aligned} B &= \frac{1}{N_{\text{links}}} \sum_{c=1}^{N_{\text{cycles}}} \frac{M_c n_c^2 + \sigma_c^2}{n_c^2 + \sigma_c^2} \\ &= \frac{1}{N_{\text{links}}} \sum_{c=1}^{N_{\text{cycles}}} \frac{1 + M_c n_c^2 / \sigma_c^2}{1 + n_c^2 / \sigma_c^2} \\ &= \frac{1}{N_{\text{links}}} \sum_{c=1}^{N_{\text{cycles}}} \frac{1 + v_c M_c}{1 + v_c}, \end{aligned} \quad (3)$$

where we have defined  $v_c = n_c^2 / \sigma_c^2$ , an up-to-now unknown parameter that quantifies the relative variability of link self-stresses within cycle  $c$ .

Two limit cases are of interest. If link tensions are approximately constant on each cycle  $c$ , we have that  $v \gg 1$  and we get

$$B = \frac{\sum_{c=1}^{N_{\text{cycles}}} M_c}{N_{\text{links}}}, \quad (4)$$

which equals the fraction of all links involved in self-stress states, or cycles. If, on the other hand, link tensions vary wildly to the point of having random signs,  $v \approx 0$ , and

$$B = \frac{N_{\text{cycles}}}{N_{\text{links}}}, \quad (5)$$

i.e., the number of cycles per link.

We later show in Sec. IV B that, for disordered cubic networks, the relevant scaling variable is  $\lambda = L\epsilon^2$ , such that link tensions are constant for  $\lambda \ll 1$  and random for  $\lambda > 1$ . These two cases are what we call, respectively, the regimes of small and large disorder.

### III. COUNTING AND MEASURING CYCLES

Appendix B enumerates general constraint-counting notions that are necessary for the calculations in this section. Here these concepts are applied to regular and disordered cubic and square networks, with and without fixed sites, to calculate the relevant properties of their cycles. This information is then used in Eq. (3) to obtain their bulk modulus in each case.

#### A. Regular networks

To begin, let us consider a regular ( $\epsilon = 0$ ) square or cubic network with periodic boundaries in the absence of fixed sites. Each line (ring actually, because of PBCs) of  $L$  collinear links is a cycle because it can support self-stresses. Thus, the network has  $dL^{d-1}$  cycles with mass  $M_c = L$  each. Furthermore, in the absence of disorder, all links on a line sustain the same exact self-stress, and therefore  $v = n_c^2 / \sigma_c^2 \rightarrow \infty$ . Using (3), we obtain

$$B = \frac{dL^{d-1}}{dL^d} L = 1. \quad (6)$$

The addition of any number of fixed sites for zero disorder does not change this result, as under homogeneous link expansion all sites remain in their original locations anyway. In

other words,  $B = 1$  for zero disorder, with any arbitrary set of fixed sites.

#### B. Disordered networks without fixed sites

The above calculation does not hold for nonzero  $\epsilon$ , no matter how small. The reason for this is that when sites are disordered, a closed line of nonaligned consecutive links no longer makes an independent cycle. While perfectly aligned links are a *degenerate* configuration and can sustain a self-stress, this ceases to be valid when sites are misaligned, even if only slightly so, as argued previously. With disorder, the remaining number of cycles is  $d$ , as shown previously on constraint-counting grounds. Thus a fraction  $d/(dL^{d-1})$  of all cycles disappears when  $\epsilon \neq 0$  and arbitrary small. Assuming, as it seems valid for arbitrarily small disorder, that  $v \rightarrow \infty$  also in this case, the bulk modulus will be reduced by the same fraction, so we obtain

$$B \sim L^{-(d-1)}, \quad (7)$$

which is valid for periodic networks with arbitrarily small but nonzero disorder.

#### C. Fixing sites

Fixing an arbitrary set of sites has the effect of removing some degrees of freedom from  $N_{\text{dof}}$  in Eq. (B1), thus inducing new cycles without simultaneously producing new flexes (as a degeneracy does). Each fixed site removes  $d$  degrees of freedom, thus inducing  $d$  new cycles, see Fig. 1. Studying the effect of fixing sites is only relevant for disordered networks since, as argued already, a regular network with PBC has all its links in cycles and thus  $B = 1$ , no matter if some sites are fixed or not.

When  $N_{\text{fixed}}$  sites are fixed, Eq. (B1) is modified to read

$$N_{\text{flexes}} = N_{\text{dof}} - dN_{\text{fixed}} - N_{\text{constr}} + N_{\text{redund}}. \quad (8)$$

Let us first consider the case of fixed lines and planes of sites.

#### D. Networks with fixed boundaries

Assume that, on a square network, any two perpendicular lines of sites are fixed, as shown in Fig. 1(a). Because of periodicity, this is equivalent to having rigid boundaries surrounding the lattice. In this case, all  $2L$  flexes of the system are eliminated and  $2L$  cycles are created, which persist for nonzero disorder. Each line of site can sustain a stress, basically independently from one another when  $\epsilon$  is small. This network thus has  $2L$  cycles, each of mass  $M_c = L$ . Similarly, if three perpendicular planes of sites are fixed on a cubic network, a system with rigid boundaries is obtained, which has  $3L^2$  cycles, each being a line of mass  $L$ . So, generally, by fixing boundaries, we obtain  $dL^{(d-1)}$  persistent cycles, each of mass  $M_c = L$ .

Using (3), we can now write

$$\begin{aligned} B &= \frac{1}{N_{\text{links}}} \sum_{c=1}^{N_{\text{cycles}}} \frac{1 + v_c M_c}{1 + v_c} \\ &= \frac{1}{dL^d} dL^{(d-1)} \frac{1 + v_c L}{1 + v_c} = \frac{1/L + v_c}{1 + v_c}. \end{aligned} \quad (9)$$

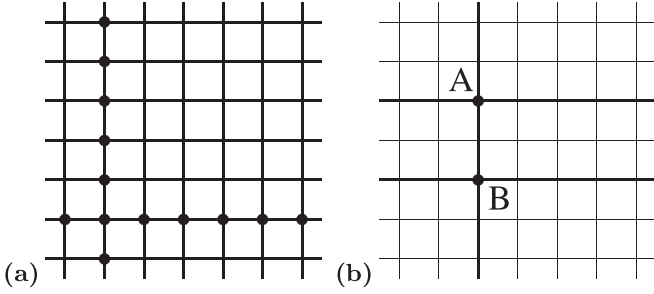


FIG. 1. These 6 x 6 grids with periodic boundaries illustrate how cycles (independent subsets of self-stressed links—thick lines) are induced on cubic and square networks with weak hot-solid disorder when some sites (black circles) are fixed. If a (horizontal or vertical) line contains a single fixed site, all links on this line can be subjected to the same self-stress and thus belong to a cycle. Each fixed site induces  $d$  new cycles. (a) Fixed boundaries are imposed in two dimensions by fixing an entire row and column of sites, in which case all links belong to some cycle. In three dimensions, fixed boundaries are obtained by fixing all sites on three orthogonal planes. For boundaries of this sort, the scaling dimension of fixed sites is  $\theta = d - 1$ , and there is a total of  $dL^{(d-1)}$  cycles, each with mass  $L$  (the number of links in the cycle). (b) In this example, two sites  $A$  and  $B$  have been fixed, inducing four cycles: two on horizontal lines, each with mass  $L = 6$ , plus two vertical cycles limited by nodes  $A$  and  $B$ , with masses, respectively, 2 and 4. The self-stress can be independently specified for all links in each cycle. Notice that the above only holds for networks with nonzero disorder. On regular networks with PBC, there are  $dL^{d-1}$  cycles, each of mass  $L$ , so all links are in cycles.

When  $\epsilon \rightarrow 0$ , all stresses are the same on each line and thus  $\nu \rightarrow \infty$ . In this limit,  $B \rightarrow 1$ , which is the same result (6) that holds for regular networks with  $\epsilon = 0$ . Disordered networks with fixed boundaries, therefore, have a continuous bulk modulus as  $\epsilon \rightarrow 0$ .

In the limit of large disorder (more on what is meant by this later), stresses on each cycle vary wildly, being both positive and negative. In this limit,  $\nu \rightarrow 0$  and we obtain  $B = 1/L$ .

Since the scaling dimension of fixed sites is  $\theta = d - 1$  in both cases considered here, we can write that for large disorder the bulk modulus scales as  $L^{-\mu_{\text{large}}}$  with  $\mu_{\text{large}} = d - \theta = 1$ , and for small disorder as  $L^{-\mu_{\text{small}}}$  with  $\mu_{\text{small}} = d - \theta - 1 = 0$ .

Now consider fixing three mutually perpendicular lines of sites in a cubic lattice, i.e., a fixed set with scaling dimension  $\theta = 1$  in space dimension  $d = 3$ . This removes  $2L$  flexes on each of three mutually perpendicular planes ( $6L$  flexes in total), thus introducing  $6L$  cycles, each of mass  $L$ . In three and larger dimensions ( $d > 3$  was not studied numerically in this paper), this result would read  $N_{\text{cycles}} = d(d - 1)L^{(d-2)}$ , each with mass  $L$ . The bulk modulus is then, according to (3),

$$B = (d - 1) \frac{1/L^2 + \nu_c/L}{1 + \nu_c}, \quad (10)$$

which holds when  $d$  mutually perpendicular lines of sites are fixed in  $d > 2$  dimensions. Again, for  $\epsilon \rightarrow 0$  we have that  $\nu \rightarrow \infty$  and thus  $B \sim 1/L$ , while for large disorder  $\nu \rightarrow 0$

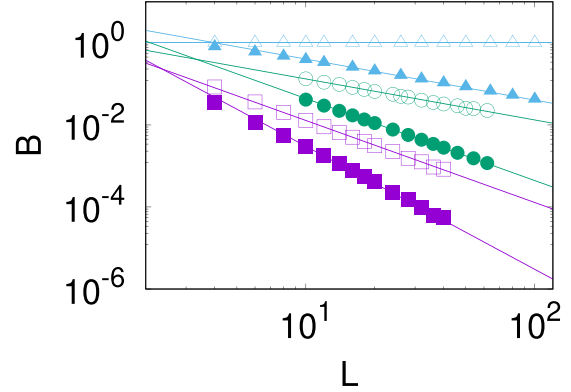


FIG. 2. Bulk compressive modulus  $B$  versus linear size  $L$  of cubic networks with periodic boundary conditions for small ( $\epsilon^2 \ll 1/L$ , empty symbols) and large ( $\epsilon^2 > 1/L$ , full symbols) disorder  $\epsilon$ . Data for three regular sets of fixed sites with scaling exponent  $\theta$  are shown in this figure: (a) No fixed sites ( $\theta = 0$ , triangles), (b) three perpendicular lines of fixed sites ( $\theta = 1$ , circles), and (c) three perpendicular planes of fixed sites ( $\theta = 2$ , squares). Full lines are power-law fits with fixed decay exponents, respectively, 0, 1, 2, and 3, as given by (16).

and  $B \sim 1/L^2$ . Also for this case we conclude that  $\mu_{\text{small}} = d - \theta$  and  $\mu_{\text{large}} = d - \theta - 1$ .

For cubic networks, these results imply that the scaling exponent  $\mu$  should take the values 2, 1, and 0 for small  $\epsilon$ , and 3, 2, and 1 for large  $\epsilon$ , respectively, for PBCs (no fixed sites), three lines of fixed sites, and three planes of fixed sites (or fixed boundary conditions). This is well verified numerically, as Fig. 2 shows.

### E. Fractal set of fixed sites

Let us consider a more general situation. Assume that, on a disordered ( $\epsilon \neq 0$ ) square or cubic network of linear extension  $L$ , composed of  $L^d$  sites with PBCs, a number  $aL^\theta$  of randomly chosen sites of the bulk are fixed, with  $0 < a < 1$  and  $0 \leq \theta \leq d$ . Each contiguous set of (approximately, because of disorder) collinear links delimited by one or more fixed sites constitutes a new cycle. Each fixed site induces  $d$  cycles on mutually perpendicular lines, so we have that a system with  $aL^\theta$  fixed sites has a total number of cycles  $adL^\theta$ , ignoring the small number  $d$  of initial cycles that already exist in the absence of fixed sites.

The typical mass of these cycles can be calculated as follows. The global density of fixed sites is  $\rho_{\text{fixed}} = aL^{-(d-\theta)}$ . Thus, on average, a line of  $L$  sites will have  $N_L^{\text{fxd}} = L\rho_{\text{fixed}} = aL^{-(d-\theta-1)}$  fixed sites. Figure 1(b) shows an example in which two sites have been fixed on the same column. The distribution of the number  $k$  of fixed sites on a given line is binomial:

$$P_k = \binom{L}{k} (\rho_{\text{fixed}})^k (1 - \rho_{\text{fixed}})^{(L-k)}. \quad (11)$$

If a line has  $k$  fixed sites on it, then it has  $k$  cycles. We will assume that fixed sites are roughly equidistant along the line, so the typical mass of each cycle can be taken to be  $M_c = L/k$ , which obviously only holds for  $k > 0$ . The case  $k = 0$  need not be considered since in this case there are no cycles (for

nonzero disorder) on this line, and thus no contribution to the bulk modulus  $B$ .

Using (3) and for a given set  $\{k_l\}$  of numbers of fixed sites on each line  $l = 1, 2, \dots, dL^{(d-1)}$ , we have that

$$\begin{aligned} B(\{k_l\}) &= \frac{1}{N_{\text{links}}} \sum_{l=1}^{dL^{(d-1)}} (1 - \delta_{k_l}^0) k_l \frac{1 + (L/k_l)\nu}{1 + \nu} \\ &= \frac{1}{dL^d} \sum_{l=1}^{dL^{(d-1)}} (1 - \delta_{k_l}^0) \frac{k_l + L\nu}{1 + \nu}, \end{aligned} \quad (12)$$

where we have made a simplifying assumption that  $\nu$  is the same for all cycles. We have written the sum over cycles as a sum over lines with nonzero  $k$ , with a multiplier  $k_l$  that accounts for the number of cycles on line  $l$ , each with mass  $M_c = L/k_l$ . Taking averages over the distribution of  $k_l$ :

$$\begin{aligned} \langle B \rangle &= \frac{dL^{(d-1)}}{dL^d} \left\{ \frac{\langle k_l \rangle + L\nu}{1 + \nu} - P_0 \frac{L\nu}{1 + \nu} \right\} \\ &= \frac{\rho_{\text{fixed}} + \nu(1 - P_0)}{1 + \nu}. \end{aligned} \quad (13)$$

For small  $\epsilon$ , each cycle is essentially a straight line and therefore all links in a cycle suffer the same stress, in which case  $\nu \rightarrow \infty$  and  $B = (1 - P_0)$ . For large disorder, stresses of random signs exist on links of a cycle and thus  $\nu \rightarrow 0$ , resulting in  $B = \rho_{\text{fixed}}$ . Therefore,

$$\langle B \rangle = \begin{cases} (1 - P_0) & \text{for small } \epsilon \\ \rho_{\text{fixed}} & \text{for large } \epsilon. \end{cases}$$

Given that  $P_0 = (1 - \rho_{\text{fixed}})^L = (1 - aL^{-(d-\theta)})^L$ , we have that, for large  $L$ ,

$$(1 - P_0) \approx \begin{cases} 1 & \text{if } \theta \geq (d - 1) \\ N_L^{\text{fxd}} & \text{if } \theta < (d - 1), \end{cases} \quad (14)$$

and, therefore,

$$\langle B \rangle = \begin{cases} 1 & \text{small } \epsilon, \theta \geq (d - 1) \\ N_L^{\text{fxd}} = aL^{-(d-\theta-1)} & \text{small } \epsilon, \theta < (d - 1) \\ (N_L^{\text{fxd}}/L) = aL^{-(d-\theta)} & \text{large } \epsilon. \end{cases} \quad (15)$$

Our results for the scaling exponent  $\mu$  in  $B \sim L^{-\mu}$  in this entire section can be condensed in the following form. If the set of fixed sites scales as  $L^\theta$ , the bulk modulus  $B$  scales as  $L^{-\mu}$  small for small disorder, and as  $L^{-\mu}$  large for large disorder, where

$$\begin{aligned} \mu_{\text{small}} &= \max\{0, (d - \theta - 1)\}, \\ \mu_{\text{large}} &= (d - \theta). \end{aligned} \quad (16)$$

Notice that this result holds, at least for the cases discussed in this section, irrespectively of how fixed sites are distributed in the network, and only depends on the scaling exponent  $\theta$  of fixed sites.

#### IV. NUMERICAL RESULTS

To test the theoretical predictions in previous sections, we provide here numerical simulations made on different kinds of networks.

#### A. Scaling exponent $\mu$

The bulk modulus  $B$  was numerically calculated for a variety of square and cubic disordered spring networks, with the help of a conjugate gradient (CG) CITE algorithm. As already noted [36], the amount of numerical work needed to obtain a solution increases very fast for  $\epsilon \rightarrow 0$  whenever there are remaining flexes in the regular network. For small  $\epsilon$ , a naive CG algorithm no longer converges for moderate sizes. This turns out to be due to the fact that the equilibrium deformation  $\langle (\delta\vec{r})^2 \rangle$  diverges as  $1/\epsilon^2$  in this limit. Analytical considerations (to be presented elsewhere) allow one to calculate the leading  $1/\epsilon$  behavior in a small- $\epsilon$  expansion of the equilibrium solution. This allowed us to start the iterative procedure from the approximate analytical solution resulting from the small- $\epsilon$  expansion, which is very close to the true solution, thus greatly improving numerical convergence times for small disorder. In this way, we obtained small-disorder results for regimes that would otherwise be inaccessible using a naive CG algorithm. After sample averaging, we obtained  $B$  as a function of  $L$  and  $\epsilon$  for each boundary condition.

Let us start by describing the cases in which fixed sites are confined to lines or planes. Figure 2 shows the bulk modulus versus size for cubic networks with PBCs and no fixed sites ( $\theta = 0$ , triangles), fixed sites along three edges ( $\theta = 1$ , circles), and fixed sites on three planes ( $\theta = 2$ , squares), in the limits of small ( $L\epsilon^2 \ll 1$ , empty symbols) and large ( $L\epsilon^2 > 1$ , full symbols) disorder. In these cases, 16 predicts that  $\mu$  must take the values 0, 1, 2, and 3. Full lines in Fig. 2 are fits using a power law where the exponent is fixed and given by 16, and only the prefactor is adjusted. As shown in the figure, very good consistency with analytical predictions is found.

Now we consider fixed sites that, instead of being confined to lines or planes, are randomly scattered in the bulk, that is, their embedding dimension equals  $d$ . We do this for both square and cubic networks. So, for  $d = 2$  and  $d = 3$  we calculate numerically the bulk modulus for several values of the size  $L$  and for several values of  $\theta$  ranging between 0 and  $d$ . This is done both for small and large disorder.

These numerical results for  $B$  versus  $L$  are then fitted using  $B \sim CL^{-\mu}$ , where now both  $C$  and  $\mu$  are fitting variables. Figure 3 shows the fitted decay exponent  $\mu$  versus  $\theta$  in two and three dimensions, in the regimes of small and large disorder. The consistency with (16), indicated by the dashed lines, is again very good.

#### B. Identification of small and large disorder regimes

In Figs. 4–6, we present numerical results for the bulk modulus  $B$  in the cases of fractal sets of fixed sites randomly scattered in the bulk, no fixed sites, fixed lines, and fixed planes of sites. Figure 4 shows the size-scaling behavior of the bulk modulus versus size  $L$ , for several values of the disorder  $\epsilon$ . These plots clearly show that  $B$  decays initially with an exponent  $\mu_{\text{small}}$  for small  $L$ , crossing over to a larger exponent  $\mu_{\text{large}}$  for  $L > L_0(\epsilon)$ , as predicted analytically. The results in Fig. 4 can be fitted rather well (dashed lines) using

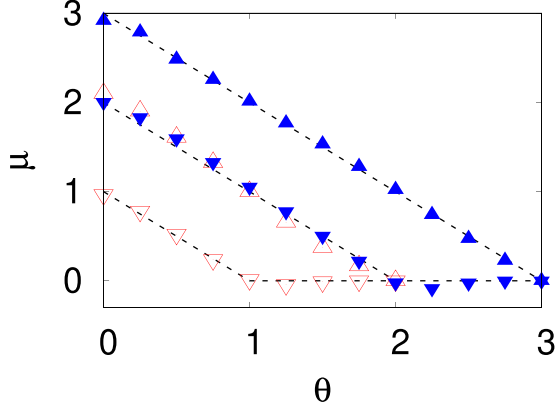


FIG. 3. Numerically fitted decay exponent  $\mu$  of the bulk modulus  $B \sim L^{-\mu}$  versus fractal dimension  $\theta$  of the set of fixed sites, for cubic (full triangles—blue online) and square (empty triangles—red online) networks, in the limits of large ( $L\epsilon^2 > 1$ , upward-pointing triangles) and small ( $L\epsilon^2 \ll 1$ , downward-pointing triangles) disorder. Dashed lines show our theoretical predictions for this exponent, which are given by Eq. (16).

the empirical expression

$$B(L, \epsilon) = \frac{B_0}{L^{\mu_{\text{small}}} + cL^{\mu_{\text{large}}}}, \quad (17)$$

where  $\mu_{\text{small}}$  and  $\mu_{\text{large}}$  are fixed and given by (16), while  $B_0$  and  $c$  are fitting constants that depend on  $\epsilon$ . This can be rewritten as

$$B(L, \epsilon) = B_0 L^{-\mu_{\text{small}}} \frac{1}{1 + (L/L_0)^{\Delta\mu}}, \quad (18)$$

where we have defined  $\Delta\mu = \mu_{\text{large}} - \mu_{\text{small}}$  and  $B_0/c = L_0^{\Delta\mu}$ . Here  $L_0(\epsilon)$  is a crossover length beyond which  $B$  decays as  $L^{-\mu_{\text{large}}}$ . Our results for  $L_0$  from numerical fits indicate that this crossover length diverges as an inverse power of  $\epsilon$  for  $\epsilon \rightarrow 0$ . Furthermore,  $B_0$  is found to be roughly constant for  $\epsilon < 10^{-2}$ . For later use, we notice that, for small  $\epsilon$  and  $L/L_0 \ll 1$ , (18) can be expanded to read

$$B(L, \epsilon) \approx B_0 L^{-\mu_{\text{small}}} (1 - (L/L_0)^{\Delta\mu}), \quad (19)$$

where  $B_0$  is a constant.

The bulk modulus versus  $\epsilon$  for fixed  $L$  is presented in Fig. 5 for several of the fixed-site sets that we studied. We fitted (lines in Fig. 5)

$$\log_{10} B(L, \epsilon) = \log_{10} B(L, 0) - m_2(L)\epsilon^2 + m_4(L)\epsilon^4 \quad (20)$$

for  $B(L, 0)$ ,  $m_2$ , and  $m_4$  to these data. Results for  $B(L, 0)$  (see Fig. 2—empty symbols) from these numerical fits are very well described by a simple power-law fit  $B(L, 0) = B_0 L^{-\mu_{\text{small}}}$ , where  $\mu_{\text{small}}$  is theoretically predicted exponent given by [Eq. (16)]  $\mu_{\text{small}} = d - \theta - 1$  for  $\theta \leq (d - 1)$ .

We can then write, for small  $\epsilon$ ,

$$B(L, \epsilon) \approx B_0 L^{-\mu_{\text{small}}} (1 - m_2 \epsilon^2), \quad (21)$$

with  $B_0$  a constant. Consistency between (19) and (21) requires that  $(L/L_0)^{\Delta\mu} = m_2 \epsilon^2$ . Therefore,  $m_2 \sim L^{\Delta\mu}$  and  $L_0 \sim \epsilon^{-2/\Delta\mu}$ . We conclude that, in the scaling regime of large  $L$  and

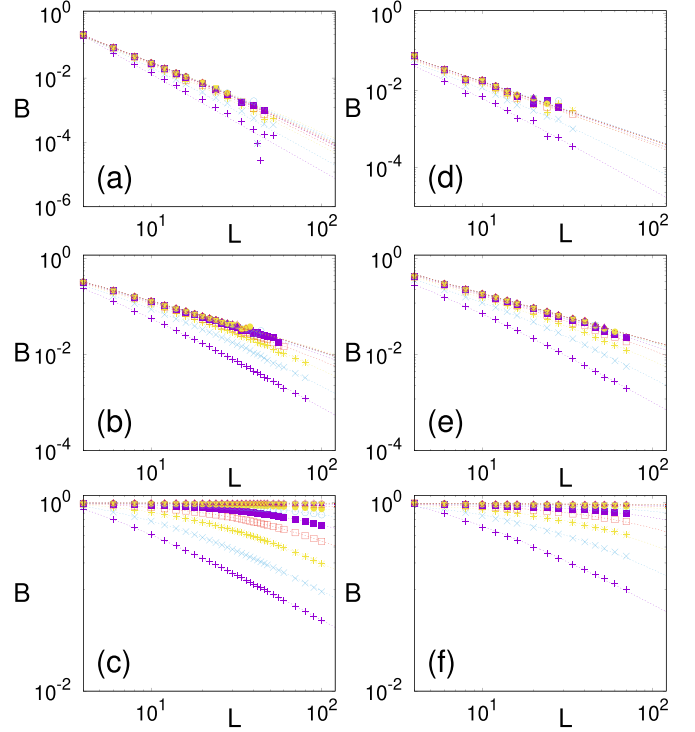


FIG. 4. Bulk modulus  $B$  of disordered cubic networks versus linear system size  $L$  for  $\epsilon = 0.33$  (pluses),  $0.23$  (crosses),  $0.16$  (asterisks),  $0.11$  (empty squares),  $0.08$  (full squares),  $0.05$  (empty circles),  $0.038$  (full circles),  $0.026$  (empty upward triangles),  $0.018$  (full upward triangles),  $0.012$  (empty downward triangles),  $0.009$  (full downward triangles),  $0.006$  (empty rhombi). The case of zero disorder, which has  $B = 1$ , is not shown. Graphs on the left column were obtained by fixing sites on boundaries, respectively, with scaling dimensions (from top to bottom)  $\theta = 0$  (no fixed sites),  $1$  (three lines are fixed), and  $2$  (three planes are fixed). Graphs on the right column were obtained by fixing a random set of bulk sites with fractal dimension (from top to bottom):  $\theta = 0.5, 1$ , and  $2$ . In all cases, dashed lines are fits for  $C_1$  and  $C_2$  of  $B(L) = C_1/(L^{\mu_{\text{small}}} + C_2 L^{\mu_{\text{large}}})$  to the numerical data, where  $\mu_{\text{small}}$  and  $\mu_{\text{large}}$  are fixed and equal to the theoretical values given by (16).

small  $\epsilon$ ,  $B(L, \epsilon) \times L^{\mu_{\text{small}}}$  should only depend on the scaling variable

$$\lambda = \epsilon^2 L^{\Delta\mu} \sim (L/L_0)^{\Delta\mu}. \quad (22)$$

This is satisfied by our numerical results, as shown in Figs. 6 and 7. Figure 6 shows that  $B$  can be written as

$$L^{-\mu_{\text{small}}} g(\epsilon^2 L^{\Delta\mu}). \quad (23)$$

The scaling function  $g(x)$  behaves as a constant when  $x \rightarrow 0$  and decays as  $1/x$  for large  $x$ . This results in  $B(L, \epsilon) \sim L^{-\mu_{\text{small}}}$  for  $\epsilon^2 L^{\Delta\mu} \ll 1$  and  $B(L, \epsilon) \sim L^{-\mu_{\text{large}}}$  for  $\epsilon^2 L^{\Delta\mu} \gg 1$ .

For the systems studied in this paper, disorder is then small whenever  $\epsilon^2 L^{\Delta\mu} \ll 1$  and large whenever  $\epsilon^2 L^{\Delta\mu} \gg 1$ . Notice that  $\Delta\mu = 1$  for  $\theta \leq (d - 1)$ , which is the case of all plots in Fig. 6. In Fig. 7, we present scaling results for  $\theta > d - 1$  in which case  $\Delta\mu < 1$  and goes to zero as  $\theta \rightarrow d$ . These results

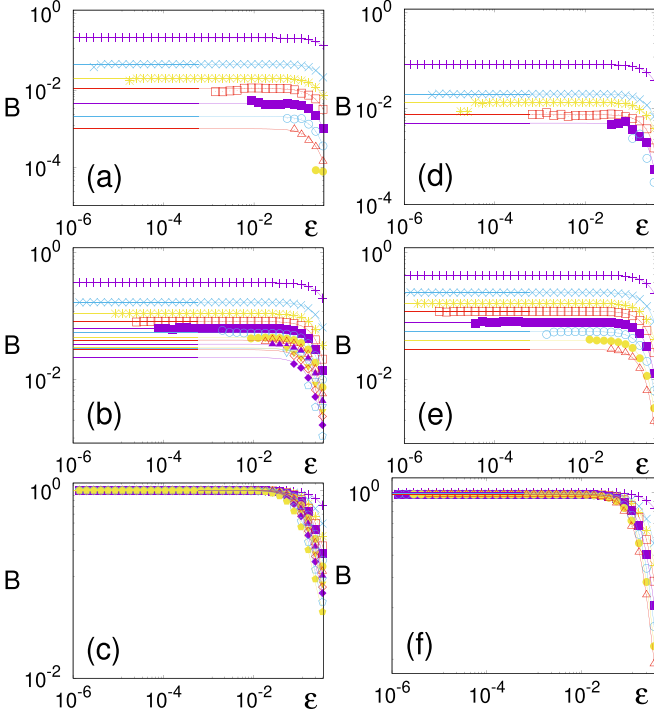


FIG. 5. Bulk modulus  $B$  versus disorder  $\epsilon$ , for  $L = 4$  (pluses), 8 (crosses), 12 (asterisks), 16 (empty squares), 20 (full squares), 24 (empty circles), 28 (full circles), 32 (empty upward triangles), 36 (full upward triangles), 40 (empty downward triangles), 44 (full downward triangles), 48 (empty rhombi), 56 (full rhombi), 70 (empty pentagons), and, 90 (full pentagons). Graphs on the left column were obtained by fixing sites on boundaries, respectively, with scaling dimensions (from top to bottom)  $\theta = 0$  (no fixed sites), 1 (three lines are fixed), and 2 (three planes are fixed). Graphs on the right column were obtained by fixing a random set of bulk sites with fractal dimension, respectively, with scaling dimensions (from top to bottom):  $\theta = 0.5, 1$ , and 2. Full lines are fits using the empirical expression (20).

show that  $B$  scales also in this regime. In the extreme case  $\theta = d$ ,  $B$  no longer depends on size.

## V. DISCUSSION

We have considered the bulk compressive modulus  $B \sim L^{-\mu}$  of cubic networks with hot-solid disorder with strength  $\epsilon$ , which are isostatic, by analytical and numerical means. By adding a nonextensive number  $\sim L^\theta$  of excess constraints in  $d$  dimensions, we obtained asymptotically isostatic networks in which the departure from true isostaticity is quantified by  $\theta$ . For these, the decay exponent  $\mu$  takes  $\theta$ -dependent values between 0 and  $d$  that are given by (16) for the limits of small and large disorder. To arrive at these results, an approximate analytical expression (3) was derived. This gives  $B$  in terms of the mass and number of cycles, plus a measure  $\nu$  of the relative variability of link tensions within a cycle.

Counting and measuring cycles under various conditions is not difficult for cubic systems, so one is left with a formula in which the only remaining unknown is  $\nu$ , i.e., the inverse link tension variability defined in Sec. II. Although we do not know the exact dependence of  $\nu$  on  $L$  and  $\epsilon$ , some amount of guessing aided by numerical results allowed us to conclude

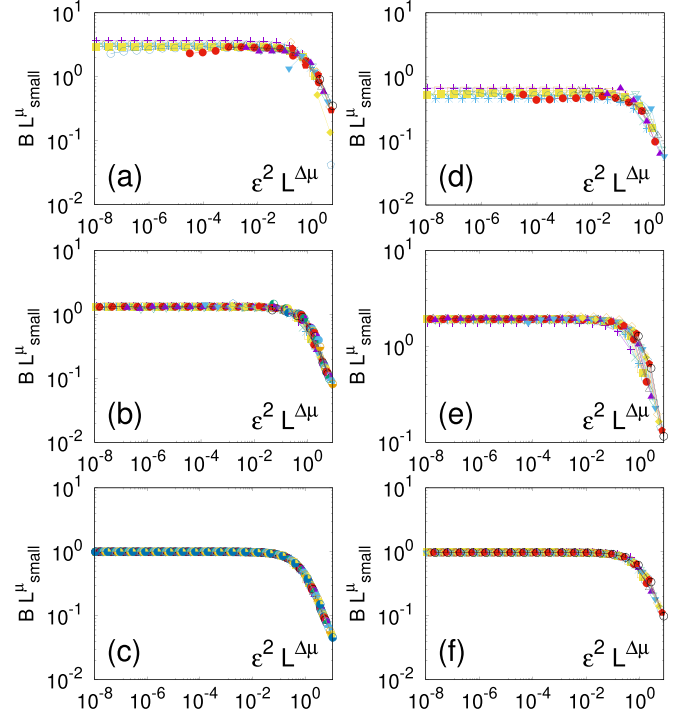


FIG. 6. Data collapse: Bulk modulus  $B$  times  $L^{\mu_{\text{small}}}$  versus scaling variable  $\lambda = \epsilon^2 L^{\Delta\mu}$  for all  $\epsilon$  and  $L$  values used in Figs. 4 and 5. Graphs on the left column were obtained by fixing sites on boundaries, respectively, with scaling dimensions (from top to bottom)  $\theta = 0$  (no fixed sites), 1 (three lines are fixed), and 2 (three planes are fixed). Graphs on the right column were obtained by fixing a random set of bulk sites with fractal dimension (from top to bottom):  $\theta = 0.5, 1$ , and 2. All results in this figure are for  $\theta \leq d - 1$ , in which case  $\Delta\mu = \mu_{\text{large}} - \mu_{\text{small}} = 1$  [see Eq. (16)].

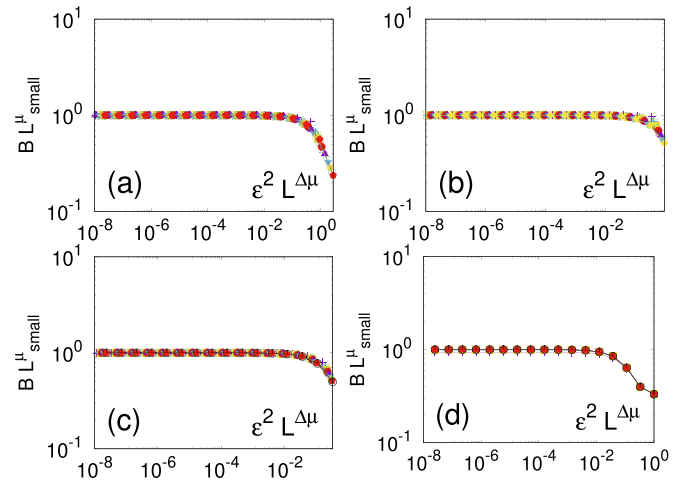


FIG. 7. Data collapse: Bulk modulus  $B$  times  $L^{\mu_{\text{small}}}$  versus scaling variable  $\lambda = \epsilon^2 L^{\Delta\mu}$  for all  $\epsilon$  and  $L$  values used in Figs. 4 and 5. All plots are for a random set of bulk fixed sites with fractal dimension  $\theta$  such that  $d - 1 \leq \theta \leq d$ . For these plots,  $\theta > d - 1$ , in which case  $\Delta\mu = \mu_{\text{large}} - \mu_{\text{small}} = d - \theta < 1$  [see Eq. (16)]. Values of  $\theta$  are 2.25 (top left), 2.50 (top right), 2.75 (bottom left), and 3.00 (bottom right).



that there are two extreme regimes, respectively,  $L^{\Delta\mu}\epsilon^2 \ll 1$ , where link tensions on each cycle are approximately constant so  $\nu \rightarrow \infty$ , and  $L^{\Delta\mu}\epsilon^2 \gg 1$ , in which link tensions vary wildly and therefore  $\nu \rightarrow 0$ . The bulk modulus scales to zero with different exponents  $\mu_{\text{small}}$  and  $\mu_{\text{large}}$  in the regimes of small and large disorder, and these exponents differ by  $\Delta\mu = 1$ , for  $\theta \leq d - 1$  and  $\Delta\mu = d - \theta$  when  $\theta > d - 1$  [see (16)]. Notice that large disorder is not intended to mean that  $\epsilon$  itself is large, but that  $1 \gg \epsilon > 1/\sqrt{L}$ .

These results imply the existence of an elastic length scale  $L_0(\epsilon)$ , which diverges in the limit of small  $\epsilon$ . Elastic properties only display their true asymptotic behavior if the system length  $L$  is much larger than this scale [6,7]. In connection with this observation, notice that  $B$  can be written in terms of the scaling variable  $\lambda = L\epsilon^2$  as  $B(L, \epsilon)L^{\mu_{\text{small}}} = g(\lambda)$  for  $0 \leq \theta \leq d$ , as Figs. 6 and 7 show. The scaling function  $g(\lambda)$  is a constant for  $\lambda \rightarrow 0$  and decays as  $1/\lambda$  for  $\lambda \gg 1$ . Other elastic properties, not discussed here, were numerically found to also scale as a function of  $\lambda$ . The way in which these results were justified analytically demonstrates that for  $L \gg L_0 = \epsilon^{-2/\Delta\mu}$ , link tensions vary randomly in sign, despite the fact that the system is subjected to homogeneous compression. This wild variation in link tensions is certainly remarkable as one could naively expect a compressive load to induce mostly compressive link tensions, but this is certainly not the case. Notice again that an amount of disorder as small as  $\epsilon_0 \sim L^{-\Delta\mu/2}$  is enough for this random stress variation to take place.

Another important conclusion follows from Fig. 4: whenever  $\theta < d - 1$ ,  $B$  does not converge to one when  $\epsilon \rightarrow 0$  but decays as  $L^{-\mu_{\text{small}}}$ , even though  $B = 1$  for  $\epsilon = 0$  exactly.  $B$  is then discontinuous at  $\epsilon = 0$  when  $\theta < d - 1$ , for any value of  $L$ . This discontinuity can be explained by noticing that only self-stressed subgraphs (or cycles) contribute to the bulk modulus [see Eq. (3)]. The regular network with  $\epsilon = 0$  is in a degenerate configuration and, because of this, it has  $dL^{d-1}$  cycles, resulting in  $B = 1$  [Eq. (6)]. However, for any nonzero amount of disorder, no matter how small, only  $d$  cycles remain. In this case, Eq. (3) gives  $B \sim L^{-(d-1)}$  [Eq. (7)] when  $\epsilon \rightarrow 0$ . The discontinuity in  $B$  results from a discontinuity in the number of cycles, which in turn is a consequence of the fact that the regular network sits on an unstable degenerate configuration. A toy model shown in Fig. 8 (right) illustrates at a basic level this effect of degeneracies. When the two bars are aligned, so the system is in a degenerate configuration, a horizontal motion of the walls relative to one another would be opposed by bar tensions, and the elastic response is nonzero. On the other hand, if the bars are only slightly misaligned, the system is no longer degenerate and thus the elastic response is zero.

For the general case of  $d$ -dimensional isostatic networks considered here, the elastic response in the presence of disorder does not become zero but very small and decreases with size. This comes about due to a proliferation of soft modes, which is explained as follows. Although a large number of flexes technically disappear from the system for nonzero disorder (see Appendix B), they still have a residual effect on the bulk modulus of the disordered network. A collective motion of a line of collinear sites is defined to be a flex if the

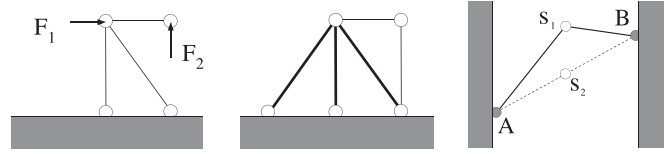


FIG. 8. Left: This network is underconstrained, as it has four degrees of freedom (two per site) but only three constraints (links). For it,  $F_1$  is an admissible load but  $F_2$  is not. The network thus has a flex, which is the vertical motion of the site held by only one spring. Any (infinitesimal) spring deformation is realizable on this network. Center: A network with unrealizable spring deformations, e.g., any such in which the vertical thick line increases its length and the lateral thick lines diminish theirs. A cycle is formed by the thick lines, which can be under stress in equilibrium in the absence of external load. This network has four degrees of freedom and five constraints, and is therefore overconstrained or hyperstatic. Right: Point  $s$  has two degrees of freedom and two constraints. Thus  $N_{\text{cycles}} = N_{\text{flexes}}$  as explained in Appendix B. In position  $s_1$  any force acting on  $s$  can be supported by link tensions, so  $N_{\text{flexes}} = 0$  and link tensions are zero in the absence of external load so  $N_{\text{cycles}} = 0$ . This network is statically ( $N_{\text{cycles}} = 0$ ) and kinematically ( $N_{\text{flexes}} = 0$ ) determinate [15]. When in position  $s_2$ , a degeneracy arises. Site  $s$  can be displaced perpendicularly to its links, thus  $N_{\text{flexes}} = 1$ . Furthermore there is a possible state of equilibrated self-stress in which both links are equally tensioned in the absence of external forces, thus  $N_{\text{cycles}} = 1$ . This network is both statically ( $N_{\text{cycles}} \neq 0$ ) and kinematically ( $N_{\text{flexes}} \neq 0$ ) indeterminate.

forces opposing this motion are exactly zero. For small  $\epsilon$ , all link tensions opposing these collective motions, while being nonzero, will be extremely weak. This is so because forces opposing this motion will be provided by links to contiguous lines. And those, for small epsilon, are almost perpendicular to the direction of motion. Therefore, a flex (or zero mode) in zero disorder will be transformed into a soft mode whenever  $\epsilon$  is nonzero but small. These modes are softer the smaller  $\epsilon$  is. They account for a very weak elastic response under mechanical loading of the network, but one that is associated with large site displacements in equilibrium.

An entirely different situation arises when a flex is removed from a regular square or cubic network by fixing one or more of the sites on a line. After disordering this network, strong forces opposing the collective flexlike motion come from links within (not perpendicular to) the flex, since one or more of its sites are now fixed. In this case, no soft mode results when disorder is introduced. Soft modes arise only from flexes that cease to exist due to disorder, i.e., when the system moves away from a degenerate geometric configuration. If all flexes are removing from a network by fixing sites, then, after introducing disorder, no soft mode remains, and in this case the bulk modulus goes to  $B = 1$  in the limit of small disorder.

Let us make some final remarks on how to generalize some of the results presented in Sec. III E. Therein we remarked that the bulk modulus scaling exponent  $\mu$  does not depend on whether fixed sites with fractal dimension  $\theta$  are randomly scattered in the bulk or confined to lines or planes. We also explicitly calculated in Sec. III D the bulk modulus when entire lines ( $\theta = 1$ ) or planes ( $\theta = 2$ ) of fixed sites are present, and noted that the resulting scaling exponents  $\mu$  are the same as for randomly scattered sites in the bulk with the same

$\theta$ . It is not difficult to generalize these calculations for the case in which the embedding dimension  $d_E$  of fixed sites is smaller than the space dimension  $d$ . For example, one can fix sites with fractal dimension  $\theta < 1$ , all confined to three lines ( $d_E = 1$ ) or with  $\theta < 2$  on three planes ( $d_E = 2$ ). This only reduces the number of cycles by a factor of  $L^{(\theta-d_E)}$  with respect to the case of fixing full lines or planes. The result thus stays the same, i.e., the bulk exponent  $\mu$  only depends on  $\theta$  and not on the embedding dimension  $d_E$  of fixed sites. We verified this numerically for a few cases with  $d_E = 1, 2$  and  $\theta < d_E$  in three dimensions.

According to these results and in contrast to sphere packings, isostatic network glasses [46] are expected to have a negligibly small compressive modulus. This happens on any isostatic network in which disorder is not specifically chosen to limit link tensions. This property of randomly disordered isostatic networks raises the possibility [47] that self-stress minimization alone may not be enough to produce a self-organized isostatic network in melts that glassify under pressure. The elastic energy of the network will then have an additional compressive contribution, which is larger the more easily compressible the network is. It seems, in principle, possible then, that at large enough pressures, this term discourages the formation of extended isostatic networks, which are easily compressed, in favor of the more rigid hyperstatic ones.

Insofar as static hot-solid disorder provides an acceptable approximate description (ignoring entropic effects at low temperatures) for the effects of weak thermal fluctuations, our results suggest that a small nonzero temperature will destabilize a regular square network under compression. This is to be contrasted with the effects of thermal fluctuations on the shear modulus  $G$  of square networks [42,43] which are found to increase with temperature.

Summarizing, in this paper, we presented an analytical method to deal with the elastic properties of weakly disordered isostatic networks. The method relies on writing the bulk modulus  $B$  as a function of the mass and number of cycles, as well as on the relative variability of link tensions on these cycles. Simple assumptions were used for the variability of tensions on a cycle. Our numerical results are in excellent agreement with those obtained from the analytical methods presented here. The main conclusions of the numerical and analytical study can be briefly stated as follows. An observed discontinuity of  $B$  at  $\epsilon = 0$  is due to a jump in the number of self-stressed subgraphs in that limit. For nonzero disorder  $\epsilon$ ,  $B$  decays as an inverse power law of the system size  $L$ . The decay exponent  $\mu$  in  $B \sim L^{-\mu}$  is obtained analytically and validated numerically, and its dependence on the model parameters is clarified. It is shown that the scaling variable  $\lambda = \epsilon^2 L$  defines two asymptotic disorder regimes in which  $\mu$  takes different values. After a suitable size rescaling, the bulk modulus can be written as a function of  $\lambda$  alone. Our results stress the importance of considering large enough lattice sizes in order to reach the asymptotic limit.

#### ACKNOWLEDGMENTS

The authors acknowledge the use of computer time on clusters Xiuhcoatl (CGTIC) and Kukulcán (Mérida) of CIN-

VESTAV, México. G.G.N. is supported by Projects No. IN102620 from UNAM-DGAPA and No. 1564464 from CONACyT, México.

#### APPENDIX A: FORMALIZATION

For similar treatments of elastic networks see, e.g., Refs. [5,15,44]. Consider an arbitrary elastic network made of  $N$  sites  $i = 1, 2, \dots, N$  located at  $\vec{r}_i$ , with nearest-neighbor (NN) vectors  $\vec{r}_{ij} = \vec{r}_j - \vec{r}_i$ . Each NN pair is connected by a spring whose repose length  $\ell_{ij}^0$  equals  $|\vec{r}_{ij}|$ . We will refer to NN pair interactions indistinctly as links, bars, contacts, or springs. The network so built is, in the absence of external load, in static equilibrium at  $\{\vec{r}_i\}$ .

In  $d$  dimensions, each site has  $d$  degrees of freedom. The total number of positional degrees of freedom is thus  $N_{\text{dof}} = Nd$ . Let  $N_{\text{links}}$  be the number of springs in the network. We define the link versors  $\vec{e}_{ij} = \vec{r}_{ij}/|\vec{r}_{ij}|$ .

##### 1. Force matrix $\hat{\mathcal{F}}$ and cycles

If external forces  $\vec{F}_i$  (a load) act on sites, link tensions  $n_{ij}$  will be induced (compression is defined to be positive), which in equilibrium must satisfy

$$\sum_{j \in v_i} n_{ij} \vec{e}_{ij} = \vec{F}_i \text{ or } \hat{\mathcal{F}}|n\rangle = |F\rangle. \quad (\text{A1})$$

Here  $\hat{\mathcal{F}}$  is a  $N_{\text{dof}} \times N_{\text{links}}$  force matrix relating site (or node) forces  $\vec{F}_i$  to bar tensions  $n_{ij}$ . Notice that (A1) may not have a solution for arbitrary node forces  $\vec{F}_i$ . For example, a freely floating network cannot satisfy (A1) if  $\vec{F}_i$  do not satisfy  $\sum_i \vec{F}_i = 0$ . A set of forces  $\vec{F}_i$  for which a solution  $\{n_{ij}\}$  of (A1) exists for a given network is called *admissible*.

Cycles are sets of links that can be in nontrivial equilibrium under zero external site forces, i.e., nonzero tensions  $n_{ij}$  satisfying

$$\hat{\mathcal{F}}|n^c\rangle = |0\rangle. \quad (\text{A2})$$

Cycles are also known as overconstrained subgraphs, self-stressed subgraphs, self-equilibrated stresses, or sets of dependent bars in several contexts. The general solution  $n_{ij}$  for bar tensions, if it exists, is not unique whenever the network has *cycles*. If, on the other hand  $\hat{\mathcal{F}}$  has a left inverse  $\hat{\mathcal{F}}_L^{-1}$ , then  $|n\rangle = \hat{\mathcal{F}}_L^{-1}|F\rangle$  and the solution  $n_{ij}$  is unique. This only holds if the network does not have cycles, in which case it is said to be statically determinate [15].

The existence of a left inverse for an  $m \times n$  matrix requires its rank to be  $n$ . In this case, the rank has to be  $N_{\text{links}}$ , i.e., the number of springs. This can only be true if  $N_{\text{links}} \leq N_{\text{dof}}$  because the rank of an  $m \times n$  matrix cannot be larger than its smallest dimension. So, for a network to not have cycles, it cannot have more springs than degrees of freedom. This is, however, a necessary, not sufficient, condition for the existence of an inverse, for reasons (the possible existence of degeneracies) that will be discussed later on in Sec. B.

In general, spring tensions can be written as

$$|n\rangle = |n\rangle_0 + \hat{\mathcal{F}}_L^{-1}|F\rangle = \hat{\mathcal{F}}_L^{-1}|F\rangle + \sum_c |n^c\rangle, \quad (\text{A3})$$

where  $|F\rangle$  are admissible external forces and  $|n\rangle_0$  are self-stresses. These last are, as already mentioned, zero if  $\hat{\mathcal{F}}$  has rank  $N_{\text{links}}$ . Notice that, although this might not be the best numerical approach for large systems, the rank can be found by using a singular value decomposition [48].

## 2. Displacement matrix $\hat{\mathcal{D}}$ and flexes

An arbitrary site displacement  $\{\delta\vec{r}_i\}$  generates link deformations, or extensions, given by

$$\delta\ell_{ij} = \vec{e}_{ij} \cdot (\delta\vec{r}_j - \delta\vec{r}_i) \text{ or } |\delta\ell\rangle = \hat{\mathcal{D}}|\delta r\rangle, \quad (\text{A4})$$

where  $\hat{\mathcal{D}}$  is a  $N_{\text{links}} \times N_{\text{dof}}$  matrix relating link extensions to site displacements. An arbitrary set of link extensions is called *realizable* if there are site deformations  $\{\delta\vec{r}_i\}$  satisfying (A4). A *flex*, also called flexibility, isometry, deformability, soft mode, or floppy mode in different contexts, is a set of site displacements  $|\delta r^{\text{flex}}\rangle$  that is mapped to zero bar deformations by  $\hat{\mathcal{D}}$ , that is, satisfies

$$\hat{\mathcal{D}}|\delta r^{\text{flex}}\rangle = 0. \quad (\text{A5})$$

In general, site displacements can be written as

$$|\delta r\rangle = \hat{\mathcal{D}}_L^{-1}|\delta\ell\rangle + \sum_{\text{flexes}} |\delta r^{\text{flex}}\rangle, \quad (\text{A6})$$

where  $|\delta\ell\rangle$  is a realizable spring stretch.  $\hat{\mathcal{D}}_L^{-1}|\delta\ell\rangle$  the part of the site displacements that is normal to all flexes, and is the only term that contributes to the elastic energy of the network. Flexes do not exist if  $\hat{\mathcal{D}}$  has a left inverse, i.e., if its rank is  $N_{\text{dof}}$ . In this case, the network is said to be kinematically determinate [15].

A freely floating network in euclidean space has at least  $d(d+1)/2$  flexes, which correspond to rigid translations and rotations. Therefore, the rank of  $\hat{\mathcal{D}}$  can be at most  $N_{\text{dof}} - d(d+1)/2$  for this case.

## 3. Relation between $\hat{\mathcal{F}}$ and $\hat{\mathcal{D}}$

If an elastic network suffers an arbitrary infinitesimal displacement around equilibrium, the total work is zero,

$$\sum_i \delta\vec{r}_i \cdot \vec{F}_i - \sum_{ij} n_{ij} \delta\ell_{ij} = 0, \\ \langle \delta r | F \rangle = \langle \delta\ell | f \rangle, \quad (\text{A7})$$

which amounts to stating that under such displacement, the work done by external forces equals the excess energy stored in springs, i.e., the principle of virtual work [2]. Therefore,

$$\langle \delta r | \hat{\mathcal{F}} | f \rangle = \langle \delta r | \hat{\mathcal{D}}^T | f \rangle \Rightarrow \hat{\mathcal{F}} = \hat{\mathcal{D}}^T. \quad (\text{A8})$$

The elastic energy stored in the network's springs ( $k=1$ ) is

$$E = \frac{1}{2} \langle \delta\ell | \delta\ell \rangle = \frac{1}{2} \langle f | f \rangle = (DEF) \frac{1}{2} \langle \delta r | \hat{\mathbf{M}} | \delta r \rangle \\ \Rightarrow \hat{\mathbf{M}} = \hat{\mathcal{D}}^T \hat{\mathcal{D}}. \quad (\text{A9})$$

## 4. Nonadmissibility of external forces $|F\rangle$ implies flexes

For any set of bar tensions  $|n\rangle$ , adequate external forces  $|F\rangle$  can always be found that satisfy equilibrium: those given by  $\hat{\mathcal{F}}|n\rangle = |F\rangle$ . However, in general, not any set of external

forces  $|F\rangle$  is *admissible*, i.e., can be equilibrated by bar tensions  $|n\rangle$ . See Fig. 8.

**Claim:** If a network has nonadmissible external forces, it has flexes.

**Proof:** If a network has nonadmissible external force sets  $|F\rangle$ , then  $\hat{\mathcal{F}}$  does not span its image. There must then exist  $N_{\text{flexes}}$  site-displacement vectors  $|\delta r^{\text{flex}}\rangle$  such that  $\hat{\mathcal{F}}|n\rangle$  is orthogonal to  $|\delta r^{\text{flex}}\rangle$  for all  $|n\rangle$  i.e.,  $\langle \delta r^{\text{flex}} | \hat{\mathcal{F}} | f \rangle = 0$  for  $f = 1, 2, \dots, N_{\text{flexes}}$ . Therefore,  $\langle \delta r^{\text{flex}} | \hat{\mathcal{F}} = \langle 0 | \Rightarrow \hat{\mathcal{F}}^T |\delta r^{\text{flex}}\rangle = \hat{\mathcal{D}} |\delta r^{\text{flex}}\rangle = |0\rangle$ , and  $|\delta r^{\text{flex}}\rangle$  is a flex, according to (A5).

Admissible force sets are orthogonal to all flexes of a framework. For example, sets of external forces that satisfy global equilibrium for a freely floating network must be orthogonal to the flexes that represent rototranslations of the system, which amounts to saying that they must have zero resultant and torque. Admissible force sets  $|F\rangle$  are those that can be written as  $\hat{\mathcal{D}}_L^{-1}|n\rangle$  for some spring-tension vector  $|n\rangle$ .

## 5. Nonrealizability of bar deformations $|\delta\ell\rangle$ implies cycles

Notice that while any site displacement  $|\delta r\rangle$  will generate some link stretch  $|\delta\ell\rangle$ , not any  $|\delta\ell\rangle$  is compatible with the network's geometric constraints, that is, realizable. Bond stretchings  $|\delta\ell\rangle$  may exist, for which no  $|\delta r\rangle$  satisfies  $\hat{\mathcal{D}}|\delta r\rangle = |\delta\ell\rangle$ . In this case, the nonrealizable part  $\hat{\mathcal{D}}|\delta r\rangle - |\delta\ell\rangle$  of the stretch is nonzero. If spring repose lengths are forced to change by  $|\delta\ell\rangle$ , the nonrealizable part will give rise to a variation in the elastic energy stored in springs that is given by

$$\delta E^{\delta\ell} = \frac{1}{2} \min_{\{|\delta r\rangle\}} \langle \hat{\mathcal{D}}\delta r - \delta\ell | \hat{\mathcal{D}}\delta r - \delta\ell \rangle. \quad (\text{A10})$$

See Fig. 8.

**Claim:** If a network has unrealizable bar stretches, it has cycles.

**Proof:** If  $|\delta\ell\rangle$  is not realizable, there is no  $|\delta r\rangle$  satisfying  $\hat{\mathcal{D}}|\delta r\rangle = |\delta\ell\rangle$ , so  $\hat{\mathcal{D}}$  does not span its image space. There must then be  $N_{\text{cycles}}$  vectors of spring tensions  $\langle n^c |$ , which are orthogonal to  $\hat{\mathcal{D}}|\delta r\rangle$  for any  $|\delta r\rangle$ , i.e.,  $\langle n^c | \hat{\mathcal{D}} |\delta r\rangle = 0$  for  $c = 1, 2, \dots, N_{\text{cycles}}$ . Equivalently,  $\langle n^c | \hat{\mathcal{D}} = 0$ , therefore  $\hat{\mathcal{D}}^T |n^c\rangle = 0$ , for  $c = 1, \dots, N_{\text{cycles}}$ . But because of (A8), this means that  $\hat{\mathcal{F}} |n^c\rangle = 0$ , and thus  $|n^c\rangle$  is a cycle, or self-equilibrated stress, according to (A2). Therefore, there are  $N_{\text{cycles}}$  sets of self-equilibrated link tensions, and some subsets of the network are *overconstrained*.

## 6. Energy upon imposed link deformations and elastic moduli

Assume that the repose lengths of all springs are modified by a stretch (a link deformation)  $|\delta\ell\rangle$ . We may decompose

$$|\delta\ell\rangle = |\delta\ell\rangle_R + \sum_{c=1}^{N_{\text{cycles}}} \frac{\langle n^c | \delta\ell \rangle}{\langle n^c | n^c \rangle} |n^c\rangle \\ = |\delta\ell\rangle_R + \left\{ \sum_{c=1}^{N_{\text{cycles}}} \frac{|n^c\rangle \otimes \langle n^c|}{\langle n^c | n^c \rangle} \right\} |\delta\ell\rangle \\ = \hat{\mathcal{D}}|\delta r_{\text{eq}}\rangle + \hat{\mathbf{P}}_{\text{self}}|\delta\ell\rangle \\ = \hat{\mathcal{D}}|\delta r_{\text{eq}}\rangle + |\Phi\rangle, \quad (\text{A11})$$

where  $\hat{\mathbf{P}}_{\text{self}}$  is a projector onto cycles and  $|\delta\ell\rangle_R = \hat{\mathcal{D}}|\delta r_{\text{eq}}\rangle$  is the realizable part of  $|\delta\ell\rangle$ . This part does not contribute to the (minimum) energy produced by the stretch because it is canceled by site displacements once in equilibrium, so we finally get

$$E^{\delta\ell} = \frac{1}{2}\langle\Phi|\Phi\rangle = \frac{1}{2}\sum_{c=1}^{N_{\text{cycles}}}\frac{\langle n^c|\delta\ell\rangle^2}{\langle n^c|n^c\rangle}, \quad (\text{A12})$$

with  $|\Phi\rangle = \hat{\mathbf{P}}_{\text{self}}|\delta\ell\rangle$  the nonrealizable part of  $|\delta\ell\rangle$ , written as

$$|\Phi\rangle = \sum_{c=1}^{N_{\text{cycles}}}\frac{\langle n^c|\delta\ell\rangle}{\langle n^c|n^c\rangle}|n^c\rangle = \sum_{c=1}^{N_{\text{cycles}}}\langle\rho^c|\delta\ell\rangle|\rho^c\rangle,$$

where  $|\rho^c\rangle$  are normalized self-stress states. Given the minimal energy cost (A12) of a bond deformation, the corresponding modulus is written as [5]

$$\begin{aligned} Y &= \frac{2E^{\delta\ell}}{\langle\delta\ell|\delta\ell\rangle} = \sum_{c=1}^{N_{\text{cycles}}}\frac{\langle n^c|\delta\ell\rangle^2}{\langle n^c|n^c\rangle\langle\delta\ell|\delta\ell\rangle} \\ &= \sum_{c=1}^{N_{\text{cycles}}}\frac{\langle\rho^c|\delta\ell\rangle^2}{\langle\delta\ell|\delta\ell\rangle}. \end{aligned} \quad (\text{A13})$$

To calculate the bulk, or compressive, modulus  $B$  in a system with PBC, we take an homogeneous expansion of all links  $|\delta\ell\rangle = \kappa(\ell_1, \ell_2, \dots, \ell_{N_{\text{links}}})$ . Then  $\langle n^c|\delta\ell\rangle = \kappa\sum_{ij}n_{ij}^c\ell_{ij}$ , and  $\langle\delta\ell|\delta\ell\rangle = \kappa^2\sum_{ij}\ell_{ij}^2$ , so (A13) reads

$$\begin{aligned} B &= \sum_{c=1}^{N_{\text{cycles}}}\frac{(\sum_{ij}n_{ij}^c\ell_{ij})^2}{\sum_{ij}(n_{ij}^c)^2\sum_{ij}(\ell_{ij})^2} \\ &= \frac{1}{N_{\text{links}}}\sum_{c=1}^{N_{\text{cycles}}}\frac{(\sum_{ij}n_{ij}^c\ell_{ij}/\ell^2 >^{1/2})^2}{\sum_{ij}(n_{ij}^c)^2}. \end{aligned} \quad (\text{A14})$$

## APPENDIX B: CONSTRAINT COUNTING

To discuss how cycles are identified and measured in this paper, we now introduce some basic notions on constraint counting. Constraint counting, i.e., determining the balance between the number of constraints (links) and degrees of freedom (sites' positions), is relatively simple for *generic* site locations, and allows one to determine the rigid properties of a network in terms of its connectivity matrix alone, without making reference to any specific property of site locations. Loosely speaking, generic configurations are those resulting, with probability almost one, when site positions are random. For example, three points on a line is not a generic but degenerate configuration, as are four points lying on a plane. Nongeneric configurations occur with zero probability when sites are randomly located.

Constraint-counting under generic conditions is based on the following topological concepts. Each site has  $d$  positional degrees of freedom in  $d$  dimensions. A network with  $L^d$  sites thus has  $N_{\text{dof}} = dL^d$ . Each link (a rotatable spring with nonzero length) determines the distance between two sites and thus provides one constraint on the set of allowed site positions. This is the kinematic approach to the rigidity of frameworks, in which site positions are the unknowns and one

asks to what extent a given set of bar lengths determines these unknowns [8–10].

Cubic or square networks have  $dL^d$  links and therefore  $N_{\text{constr}} = dL^d$  for them. A *flex* (also a *floppy* or *soft* mode in the context of vibrational properties) is an isometry of the network, i.e., an infinitesimal transformation of site positions that keeps all link lengths unchanged. Each flex of the network implies a nonadmissible load, i.e., a load direction that cannot be equilibrated by tensions on springs. A subset of the network's sites is said to be *mutually rigid* or rigidly connected if all their relative distances are fixed by the links induced by this subset. A rigidly connected subset might still have (global) flexes, as, e.g., on Euclidean geometries,  $d + d(d - 1)/2$  rototranslations keep all intersite distances unchanged for freely floating networks. A load is admissible under such circumstances only if it has zero resultant and zero torque, i.e., it is orthogonal to all remaining flexes, as already mentioned.

If a link is added between two sites that are already mutually rigid, no new flex is removed. This link is called *redundant*, and the network so generated is said to be *overconstrained*. Each redundancy induces a new cycle, i.e., a subset of the network that can independently sustain self-stress in the absence of external load, as illustrated if one imagines that this new spring is too short or too long compared to the distance between the sites it connects. Therefore, the number  $N_{\text{redund}}$  of redundant links is exactly the number of cycles  $N_{\text{cycles}}$  that we need to know to calculate the bulk modulus.

It is important not to confuse the number of redundancies or cycles  $N_{\text{redund}}$  with the number  $M_c$  of links in a self-stressed subgraph. This confusion might sometimes result from a somewhat unfortunate use of terminology in the literature. All links in a self-stressed subgraph are sometimes said to be redundant or dependent. They may all indeed be called redundant, but only in the sense that any one of them can be removed without inducing new flexibilities. But as soon as this one is removed, all other links in the cycle cease to be redundant. Said differently, i.e., considering the addition instead of the removal of a link, the addition of a single redundant link will, in general, induce self-stress in several other links, thus one may have  $N_{\text{redund}} = 1$  but  $M_c$  will be larger than one.

The basic constraint-counting relationship linking the quantities defined above reads

$$\begin{aligned} N_{\text{flexes}} &= N_{\text{dof}} - N_{\text{constr}} + N_{\text{redund}} \\ &= N_{\text{dof}} - N_{\text{constr}} + N_{\text{cycles}}, \end{aligned} \quad (\text{B1})$$

which means that the number  $N_{\text{flexes}}$  of remaining degrees of freedom results from subtracting the number ( $N_{\text{constr}} - N_{\text{redund}}$ ) of *independent constraints*, i.e., those that effectively remove one degree of freedom, from the initial number of degrees of freedom  $N_{\text{dof}}$ .

Actually, (B1) is valid in general and not only for generic rigidity. Under generic conditions, the identification of redundant constraints, without being easy in itself, is merely a matter of studying the connectivity matrix of the network. Even in the generic case, this task is far from trivial and requires specialized graph-theoretical methods [49,50], which furthermore only work for particular circumstances. The

existence of degeneracies further complicates this task, as certain constraints may become redundant that otherwise would not be for generic configurations.

One can illustrate the effect of degeneracy by means of a trivial example in two dimensional space (see Fig. 8). Consider a single site  $s$  connected by two links to two fixed points  $A$  and  $B$ . A site in  $d = 2$  has two degrees of freedom, thus  $N_{\text{dof}}=2$ . Fixed sites have no degree of freedom by definition. Each link is a constraint and therefore  $N_{\text{constr}}=2$ . Equation (B1) then implies  $N_{\text{flexes}} = N_{\text{cycles}}$ , since  $N_{\text{redund}} = N_{\text{cycles}}$  as explained.

In a generic configuration such as  $s_1$  in Fig. 8, points  $A$ ,  $B$ , and  $s$  are not aligned. In this case, no link is redundant and therefore  $N_{\text{flexes}}=N_{\text{redund}}=0$ . Point  $s$  will in this case be rigidly fixed by its two links. There are no cycles and therefore both links are stress-free in the absence of external load on  $s$ . There are no flexes either, and therefore any force acting on  $s$  constitutes an admissible load that will be supported by adequate forces emanating from the fixed sites  $A$  and  $B$ .

A degeneracy arises whenever  $A$ ,  $B$ , and  $s$  are aligned, such as  $s_2$  in Fig. 8. In this case, point  $s$  can be infinitesimally displaced (thus,  $N_{\text{flexes}} = 1$ ) perpendicularly to the alignment line, since neither link can exert a restoring force in this direction. According to (B1), we must also have  $N_{\text{redund}} = 1$ , which implies  $N_{\text{cycles}} = 1$ . The degenerate cycle that ensues corresponds to having both links under the same arbitrary stress, a situation under which point  $s$  remains equilibrated. We thus see that while (B1) holds in both the generic and degenerate cases, degeneracies can render some links redundant, leading to the appearance of additional flexes and cycles.

Particularizing now to the case of a regular ( $\epsilon = 0$ ) cubic or square network with PBCs, which is in a degenerate configuration, we then note that each of the  $dL^{d-1}$  lines of collinear links constitutes an independent cycle. Each of these lines can carry an independent arbitrary tension  $n_c$ , the same on all of its  $L$  links, and this will be an equilibrium state in the absence of external load. According to (B1), there must also be  $dL^{d-1}$  independent flexes in this system. These are easily identified. Each line of collinear sites can be infinitesimally displaced in the direction of collinearity, since all other incoming links are normal to this motion and therefore can exert no opposing force.

However, when  $\epsilon \neq 0$  (the generic case), lines of collinear sites can no longer be freely displaced, as this motion would be opposed, if only weakly, by forces on links to contiguous lines of sites, which are no longer perpendicular to the direction of motion. Therefore, a number of flexes (and cycles) suddenly disappear from the system for any nonzero  $\epsilon$ . A few (trivial) flexes do remain, however. A rigid translation of all sites in any of the  $d$  directions is still an isometry or flex. Rotations are not isometries [44] in a network that is connected periodically along each of the  $d$  space directions (and thus has the topology of a  $d + 1$  dimensional torus). Therefore, only  $d$  flexes remain and, consequently, the disordered network still has  $d$  cycles, which we do not care to identify for the purposes of this paper (their number is finite and thus their contribution to the bulk modulus is negligible). We therefore conclude that any amount of disorder  $\epsilon$ , no matter how slight, removes  $d(L^{d-1} - 1)$  flexes and cycles from a square or cubic network with PBCs. This accounts for the observed discontinuity in the elastic modulus at  $\epsilon = 0$ .

- 
- [1] J. C. Maxwell, On the calculation of the equilibrium and stiffness of frames, *London, Edinburgh, Dublin Philos. Mag. J. Sci.* **27**, 294 (1864).
- [2] P. Nagarajan, *Matrix Methods of Structural Analysis*, 1st ed. (CRC Press, Taylor & Francis, Boca Raton, FL, 2019).
- [3] J. C. Phillips, Topology of covalent non-crystalline solids I: Short-range order in chalcogenide alloys, *J. Non-Cryst. Solids* **34**, 153 (1979).
- [4] C. F. Moukarzel, Isostatic Phase Transition and Instability in Stiff Granular Materials, *Phys. Rev. Lett.* **81**, 1634 (1998).
- [5] M. Wyart, On the rigidity of amorphous solids, *Ann. Phys. (Paris)* **30**, 1 (2005).
- [6] C. F. Moukarzel and G. G. Naumis, Comment on “Penrose Tilings as Jammed Solids,” *Phys. Rev. Lett.* **115**, 209801 (2015).
- [7] O. Stenull and T. C. Lubensky, Penrose Tilings as Jammed Solids, *Phys. Rev. Lett.* **113**, 158301 (2014).
- [8] L. Asimow and B. Roth, Rigidity of graphs, *Trans. Am. Math. Soc.* **245**, 279 (1978).
- [9] L. Asimow and B. Roth, Rigidity of graphs 2, *J. Math. Anal. Appl.* **68**, 171 (1979).
- [10] H. Crapo, Structural rigidity, *Struct. Topol.* **1**, 26 (1979).
- [11] L. K. Johnson, C. Richburg, M. Lew, W. R. Ledoux, P. M. Aubin, and E. Rombokas, 3d printed lattice microstructures to mimic soft biological materials, *Bioinspir. Biomim.* **14**, 016001 (2018).
- [12] D. Yan, J. Chang, H. Zhang, J. Liu, H. Song, Z. Xue, F. Zhang, and Y. Zhang, Soft three-dimensional network materials with rational bio-mimetic designs, *Nat. Commun.* **11**, 1180 (2020).
- [13] J. Chang, D. Yan, J. Liu, F. Zhang, and Y. Zhang, Mechanics of three-dimensional soft network materials with a class of bio-inspired designs, *J. Appl. Mech.* **89**, 071004 (2022).
- [14] C. Moukarzel and P. M. Duxbury, Comparison of rigidity and connectivity percolation in two dimensions, *Phys. Rev. E* **59**, 2614 (1999).
- [15] S. Pellegrino and C. R. Calladine, Matrix analysis of statically and kinematically indeterminate frameworks, *Int. J. Solids Struct.* **22**, 409 (1986).
- [16] G. H. Döhler, R. Dandoloff, and H. Bilz, A topological-dynamical model of amorphycity, *J. Non-Cryst. Solids* **42**, 87 (1980).
- [17] M. F. Thorpe, Rigidity percolation in glassy structures, *J. Non-Cryst. Solids* **76**, 109 (1985).
- [18] J. C. Phillips and M. F. Thorpe, Constraint theory, vector percolation and glass-formation, *Solid State Commun.* **53**, 699 (1985).
- [19] S. Feng and P. N. Sen, Percolation on Elastic Networks: New Exponent and Threshold, *Phys. Rev. Lett.* **52**, 216 (1984).
- [20] M. Thorpe and P. M. Duxbury, *Rigidity Theory and Applications, Fundamental Materials Research* (Kluwer Academic & Plenum Press, New York, 1999).

- [21] C. Moukarzel and P. M. Duxbury, Stressed Backbone and Elasticity of Random Central-Force Systems, *Phys. Rev. Lett.* **75**, 4055 (1995).
- [22] D. J. Jacobs and M. F. Thorpe, Generic Rigidity Percolation: The Pebble Game, *Phys. Rev. Lett.* **75**, 4051 (1995).
- [23] S. R. Nagel, Metallic glasses, in *Advances in Chemical Physics*, edited by I. Prigogine and S. A. Rice, Vol. 51 (John Wiley & Sons, Ltd., 1982), pp. 227–275.
- [24] D. Selvanathan, W. J. Bressler, and P. Boolchand, Stiffness transitions in  $\text{Si}_x\text{Se}_{1-x}$  glasses from raman scattering and temperature-modulated differential scanning calorimetry, *Phys. Rev. B* **61**, 15061 (2000).
- [25] P. Boolchand, D. G. Georgiev, and B. Goodman, Discovery of the intermediate phase in chalcogenide glasses, *J. Optoelectron. Adv. Mater.* **3**, 703 (2001).
- [26] M. V. Chubynsky and M. F. Thorpe, Self-organization and rigidity in network glasses, *Curr. Opin. Solid State Mater. Sci.* **5**, 525 (2001).
- [27] M. F. Thorpe, M. V. Chubynsky, D. J. Jacobs, and J. C. Phillips, Non-randomness in network glasses and rigidity, *Glass Phys. Chem.* **27**, 160 (2001).
- [28] P. Boolchand, M. Bauchy, M. Micoulaut, and C. Yildirim, Topological phases of chalcogenide glasses encoded in the melt dynamics, *Phys. Status Solidi B* **255**, 1800027 (2018).
- [29] N. Xu, M. Wyart, A. J. Liu, and S. R. Nagel, Excess Vibrational Modes and the Boson Peak in Model Glasses, *Phys. Rev. Lett.* **98**, 175502 (2007).
- [30] T. S. Grigera, V. Martin-Mayor, G. Parisi, and P. Verrocchio, Phonon interpretation of the 'boson peak' in supercooled liquids, *Nature* **422**, 289 (2003).
- [31] A. Huerta and G. G. Naumis, Relationship between glass transition and rigidity in a binary associative fluid, *Phys. Lett. A* **299**, 660 (2002).
- [32] G. G. Naumis and J. C. Phillips, Bifurcation of stretched exponential relaxation in microscopically homogeneous glasses, *J. Non-Cryst. Solids* **358**, 893 (2012).
- [33] J. C. Mauro, A. Tandia, K. Deenamma Vargheese, Y. Z. Mauro, and M. M. Smedskjaer, Accelerating the design of functional glasses through modeling, *Chem. Mater.* **28**, 4267 (2016).
- [34] C. F. Moukarzel, Two rigidity-percolation transitions on binary Bethe networks and the intermediate phase in glass, *Phys. Rev. E* **88**, 062121 (2013).
- [35] C. F. Moukarzel, Elastic collapse in disordered isostatic networks, *Europhys. Lett.* **97**, 36008 (2012).
- [36] C. F. Moukarzel, Elastic anomalies in disordered square networks, *J. Stat. Mech.: Theory Exp.* (2015) P04008.
- [37] C. F. Moukarzel, Random multiplicative processes and the response functions of granular packings, *J. Phys.: Condens. Matter* **14**, 2379 (2002).
- [38] C. F. Moukarzel, Random multiplicative response functions in granular contact networks, in *Challenges in Granular Physics*, edited by Thomas Halsey and A. Mehta (World Scientific, Singapore, 2003).
- [39] C. F. Moukarzel, Response functions in isostatic packings, in *The Physics of Granular Media*, edited by Haye Hinrichsen and D. E. Wolf (Wiley-VCH, Berlin, 2005), pp. 23–43.
- [40] J. M. Ziman, *Models of Disorder*, 2nd ed. (Cambridge University Press., Oxford, 1982).
- [41] A. Souslov, A. J. Liu, and T. C. Lubensky, Elasticity and Response in Nearly Isostatic Periodic Lattices, *Phys. Rev. Lett.* **103**, 205503 (2009).
- [42] M. Dennison, M. Sheinman, C. Storm, and F. C. MacKintosh, Fluctuation-Stabilized Marginal Networks and Anomalous Entropic Elasticity, *Phys. Rev. Lett.* **111**, 095503 (2013).
- [43] L. Zhang and X. Mao, Finite-temperature mechanical instability in disordered lattices, *Phys. Rev. E* **93**, 022110 (2016).
- [44] S. D. Guest and J. W. Hutchinson, On the determinacy of repetitive structures, *J. Mech. Phys. Solids* **51**, 383 (2003).
- [45] M. R. Hestenes, Methods of conjugate gradients for solving linear systems, *J. Res. Natl. Bur. Stand.* **49**, 409 (1952).
- [46] P. Boolchand, G. Lucovsky, J. C. Phillips, and M. F. Thorpe, Self-organization and the physics of glassy networks, *Philos. Mag.* **85**, 3823 (2005).
- [47] C. F. Moukarzel, Rigidity percolation in a field, *Phys. Rev. E* **68**, 056104 (2003).
- [48] S. Pellegrino, Structural computations with the singular value decomposition of the equilibrium matrix, *Int. J. Solids Struct.* **30**, 3025 (1993).
- [49] C. Moukarzel, An efficient algorithm for testing the generic rigidity of graphs in the plane, *J. Phys. A: Math. Gen.* **29**, 8079 (1996).
- [50] D. J. Jacobs and M. F. Thorpe, Generic rigidity percolation in two dimensions, *Phys. Rev. E* **53**, 3682 (1996).